Performance Evaluation of Radio Map Construction Methods for Wi-Fi Positioning Systems

Suk Hoon Jung, Byeong-Cheol Moon, and Dongsoo Han, *Member, IEEE*

***Abstract*—A radio map is a collection of signal fingerprints labeled with their collected locations. It is known that the performance of a fingerprint-based positioning systems is closely related to the precision and accuracy of the underlying radio maps. However, little has been studied on the performance of radio maps in relation to the fingerprint collection methods and the radio map models, which determine the accuracy and precision of radio maps, respectively. This paper evaluates the performance of various radio map construction methods in both indoor and outdoor environments. Four radio map construction methods, i.e., a point-by-point manual calibration, a walking survey, a semisupervised learning-based method, and an unsupervised learning-based method, have been compared. We also evaluate the performance of various types of radio map models that represent the characteristics of collected fingerprints. To demonstrate the importance of the radio map model, a new model named signal fluctuation matrix (SFM) was developed, and its performance was compared with that of the three conventional radio map models, respectively. The evaluation revealed that the performance of the radio maps was very sensitive to the design of radio map models and the number of fingerprints collected at each location. The performance achieved by SFM-based positioning was comparable with that of the other models despite using a small number of fingerprints.**

***Index Terms*—Wi-Fi positioning system, radio fingerprint, radio map construction, signal fluctuation matrix.**

I. Introduction

PEDESTRIAN navigation is an important issue in the construction of efficient multimodal transportation systems [1]. One requirement is accurate positioning of people in indoor, underground, and outdoor areas where Global Positioning System (GPS) signals are blocked. To provide accurate positioning services in GPS-denied areas, a variety of wireless positioning techniques have been studied using Wi-Fi, Ultra-Wideband (UWB), Radio-Frequency IDentification (RFID), etc. [2]. Among the wireless positioning techniques, Wi-Fi fingerprint-based positioning has attracted considerable attention because of the wide availability of Wireless Local Area Networks (WLANs) and relatively high resolution of the fingerprint-based positioning techniques [2].

A Wi-Fi fingerprint is the pattern of Received Signal Strengths (RSS) of a collection of Access Points (APs) visible at a particular location, and it is trained from RSS samples collected at a given location. A radio map is a database of fingerprints labeled with their location information for a particular building or an area. Once a radio map is constructed, a positioning algorithm can estimate a location of an online fingerprint measurement by comparing it with the fingerprints in the radio map [3]. The radio map is thus an essential component of Wi-Fi fingerprint-based positioning systems. Various radio map construction methods are available owing to the diversity of the fingerprint collection methods and radio map representation models [3].

Two research approaches in constructing radio maps have been taken. One is to reduce the fingerprint collection cost, especially with respect to the human effort required in labeling collected fingerprints with accurate locations. The collection methods have evolved from a point-by-point manual calibration [4], to a walking survey [5], semi-supervised learning-based [6]–[9], inertial sensor-based [10]–[13], and finally unsupervised learning-based radio map construction methods [14]. With the evolution of the methods, the radio map construction cost has been reduced, but the accuracy of fingerprint labeling is usually sacrificed.

The other research approach is to develop radio map model designs to represent RSS patterns as precisely as possible even if only a few training samples are given. To achieve this goal, the signal characteristics should be effectively represented in a radio map model. The radio map models are classified into deterministic or probabilistic models [3], and positioning algorithms appropriate to the models are used. The deterministic radio map models usually represent the fingerprint observed at a location with a vector of mean RSSs, whereas the probabilistic models, such as Gaussian distribution and histogram models, use the distribution of RSSs from each AP at a location. The probabilistic radio map models are known to achieve better accuracy than the deterministic models [15]. However, the construction of probabilistic radio maps usually requires a large number of fingerprint samples at each location to construct reliable RSS distributions, leading to high radio map construction cost.

Because Wi-Fi fingerprinting is a kind of pattern recognition with noisy wireless signals, the accuracy of fingerprint-based positioning methods is influenced by the precision and accuracy of the underlying radio maps. Positioning algorithms

Manuscript received November 22, 2015; revised March 18, 2016 and June 19, 2016; accepted July 14, 2016. Date of publication August 11, 2016; date of current version March 27, 2017. This work was supported in part by the Ministry of Land, Infrastructure and Transport, South Korea, under the Railway Technology Research Program supervised by the Korea Agency for Infrastructure Technology Advancement under Grant 16RTRP-B086931-03 and in part by the National Research Foundation of Korea (NRF) Grant funded by the Korean government (Ministry of Science, ICT and Future Planning) under Grants NRF-2015R1A2A1A10052224 and NRF-2015R1A5A7037751. The Associate Editor for this paper was X. Cheng. *(Corresponding author: Dongsoo Han.)*

The authors are with the Department of Computer Science, Korea Advanced Institute of Science and Technology, Daejeon 305-701, South Korea (e-mail: sh.jung@kaist.ac.kr; chul7672@kaist.ac.kr; dshan@kaist.ac.kr).

Color versions of one or more of the figures in this paper are available online at http://ieeexplore.ieee.org.

Digital Object Identifier 10.1109/TITS.2016.2594479

and systems have been extensively studied [15]–[19]. These studies provide a comprehensive overview of the technologies and the architectures of various wireless positioning methods. However, radio map construction methods have not been extensively studied. The choice of an appropriate fingerprint collection method and a radio map model would be the first step in constructing a cost-efficient, high performance fingerprint-based positioning system. More in-depth knowledge on radio map construction methods is required to make a correct choice.

This paper provides information on the performance and cost of radio map construction methods, especially for the fingerprint collection methods and radio map models. We compare the performance of four fingerprint collection methods; a point-by-point calibration, a walking survey, a semi-supervised learning-based, and an unsupervised learning-based radio map construction method. This study also evaluates the performance of several radio map models that are often used for fingerprint-based positioning.

Another goal of this paper is to introduce a new probabilistic radio map model, named Signal Fluctuation Matrix (SFM). Traditionally, probabilistic radio maps require many fingerprint samples because they investigate an RSS distribution for every AP and location, respectively. The SFM addresses this problem by constructing a universal pattern of RSSs using only a small number of fingerprint samples.

Four experiments were performed to evaluate the performance of the radio map construction methods. Three experiments were performed on the seventh floor of N1 building, and in N5 building at Korea Advanced Institute of Science and Technology (KAIST), to evaluate the performance of indoor radio maps constructed by point-by-point manual calibration, semi-supervised learning, and unsupervised learning methods. One experiment was performed to evaluate the performance of outdoor radio maps constructed by a walking survey and by two semi-supervised learning-based methods.

The experiments revealed that the radio map performance was very sensitive to the radio map models and the number of fingerprint samples collected at each location. In indoor radio maps, the SFM-based model always exhibited the best performance in accuracy when more than 10 samples were collected at each location. In addition, with numerous Wi-Fi signals in outdoor environments, the Wi-Fi positioning outperformed GPS in accuracy, indicating that it can be used to reduce the GPS positioning error, especially in urban street canyons [20].

This paper is organized as follows. Section II describes various radio map construction methods. Section III presents the proposed SFM model. Section IV describes a mapping strategy of radio maps into models and positioning algorithms depending on the density of fingerprints and fingerprint collections methods. The evaluation results are described in Section V, and we draw conclusions in Section VI.

II. Radio Map Construction Methods

A. *Fingerprint Collection and Labeling Methods*

Radio map construction usually involves fingerprint collection and location-labeling activities. Various fingerprint collection and labeling methods have been developed for Wi-Fi fingerprint-based positioning. The first is a primitive method based on point-by-point manual calibration. The primary goal of this method is to achieve the highest accuracy possible without much regard for the calibration cost. In the point-by-point manual calibration, the target area is partitioned into numerous pieces, i.e. *locations*, and then dedicated surveyors collect fingerprint samples point-by-point considering the center of each location as a measurement point [see Fig. 1(a)]. Typically, locations are sized between 2 m $\times$ 2 m to 5 m $\times$ 5 m, and dozens of samples are collected at each location [4].

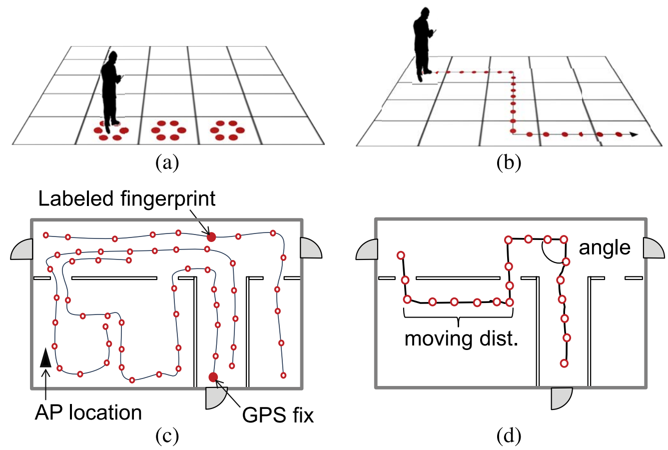

Fig. 1. Fingerprint collection and labeling methods. (a) Point-by-point calibration. (b) Walking survey. (c) Semisupervised learning. (d) Inertial sensor-based method.

As the point-by-point manual calibration requires considerable time and effort, a walking survey was used instead to reduce the effort required to recognize each location [5]. In the walking survey, the survey paths are planned in advance, but the collection points do not have to be specified [see Fig. 1(b)]. Only the specific points, such as the start, corners, and the end point of the survey paths are marked to guide the surveyors. The fingerprint samples are collected while the surveyors are walking along the paths carrying collection devices.

Although the walking survey can reduce the collection effort to some extent, it still requires considerable time and effort to construct radio maps for most of buildings all over the world. As a result, crowdsourcing approaches in which fingerprint samples are collected from numerous users, and then radio maps are constructed using the crowdsourced samples, have been proposed to reduce the cost of constructing radio maps [11]. The crowdsourced samples can be viewed as unlabeled data since the true locations at which the samples have been obtained are unknown. Therefore, the issue to address is the location-labeling of the unlabeled samples to construct radio maps.

Additional data from inertial sensors embedded in wireless devices such as a three-axis accelerometer, a compass, and a gyroscope can be used for estimating the unknown location labels [see Fig. 1(d)]. UnLoc [10], Microsoft Zee [11], LiFS [12], WILL [13], and others seek to incorporate dead-reckoning techniques for the fingerprints labeling by referring to sensing data from inertial sensors and to the location of stairs, elevators, and other features in an indoor area. These so-called inertial sensor-based methods can reduce or even eliminate manual efforts required in fingerprint labeling. However, the involvement of additional sensors impedes the contribution of fingerprint samples from numerous wireless devices because it requires additional power consumption for the sensor operation. Moreover, the sensors embedded in current wireless devices are not precise enough to correctly label the fingerprint with location information.

The unknown locations of fingerprint samples can also be estimated from their relations in the Wi-Fi signal space. This approach is similar to that used for the cooperative localization of the nodes in Wireless Sensor Networks (WSNs). WSN-based cooperative localization methods usually determine the positions of sensor nodes by organizing the nodes in the network area based on the internode measurements obtained during their communications [21], [22]. Similarly, unlabeled fingerprint samples collected in a WLAN can be organized in the network area for their location-labeling. The main difference between cooperative localization and fingerprint labeling is the target object for the positioning; cooperative localization usually estimates the current positions of sensor nodes [23], whereas fingerprint labeling deals with the signal measurements accumulated from moving devices in a training phase. As a result, the number of target objects for fingerprint labeling is usually much larger than that for cooperative positioning. To deal with such a large number of targets, advanced machine-learning techniques, such as semi-supervised learning or unsupervised learning, have been employed for fingerprint labeling.

Semi-supervised learning techniques, such as Manifold learning [6], [7], [14], [25] and expectation maximization [26], [27], can be applied for estimating the unknown locations of samples if a small number of labeled samples are given as location references. The locations of APs or GPS fixes have often been used for the location references instead of the labeled fingerprints [9]. The semi-supervised learning aims to further reduce the manual calibration cost, and it has contributed to reduction of the cost to some extent. However, it still requires some effort to acquire the location references.

There has also been an attempt to apply the unsupervised learning paradigm to construct radio maps using only unlabeled fingerprint samples [14]. It is distinguished from the semi-supervised learning-based and sensor-based methods because it does not require any explicit labeling effort or sensing data for references. The proposed method integrates a memetic algorithm and a segmental k-means algorithm in a hybrid global-local optimization scheme to find the optimal placement of unlabeled fingerprints in a partitioned indoor area [14]. However, a considerable amount of computation time is required for the optimization task. Most of the computation is required for the global search that is used to prevent the learning from being stuck into local optima.

In addition to cost reduction, the fingerprint collection and labeling methods pursue enhanced accuracy of location-labeling for fingerprints because it determines the accuracy of radio maps. A radio map constructed by a point-by-point manual calibration usually shows the best accuracy because the locations are labeled by intensive surveys. There is some loss in accuracy in the other methods due to errors included in their automation processes.

B. Radio Map Models

A high-quality radio map can be constructed if a large amount of fingerprint samples are used with accurate location-labeling. The quality is also influenced by the design of a radio map model because it determines the precision of RSS pattern representation. The model should be able to represent the characteristics of WLAN signals as precisely as possible. Otherwise, the radio map quality is limited even if a large amount of samples are used for the radio map construction. In contrast, if a radio map model is judiciously designed, it can represent the necessary characteristics of WLAN signals by using only a small number of fingerprint samples. Therefore, the choice of radio map model is critical to fully utilize the collected fingerprint samples.

Radio map models can be classified into two categories: deterministic and probabilistic. In a deterministic radio map model, usually a vector of mean RSS is used to represent a fingerprint of a location. In a probabilistic model, the characteristics of collected fingerprint samples are summarized into statistic values such as a norm and a standard deviation. The Gaussian and histogram models are well-known probabilistic radio map models [16]. The Gaussian model explains the distribution of RSSs assuming that they follow a Gaussian distribution. The average and the standard deviation are the two key parameters of the distribution. The histogram model accumulates RSSs into a histogram. If enough samples can be provided, highly detailed modeling is possible using the histogram model. We can also model a radio map using other kinds of distributions such as the log-normal distribution [28], Rayleigh distribution [29], double-peak Gaussian distribution [30], etc. We do not delve into the details in this paper, however, because the resolution of their representation is usually between those of the Gaussian and histogram models.

When only a small number of fingerprint samples have been collected at each location, a deterministic radio map model is usually considered, whereas when more than a dozen samples have been collected, a probabilistic radio map model is typically considered. Consequently, different kinds of radio map models have been used depending on the number of collected samples at each location.

The positioning algorithms that estimate locations by searching nearest fingerprints in deterministic radio maps for an online measurement, such as k-Nearest Neighbor (kNN) and weighted kNN, belong to the deterministic positioning algorithm category. The positioning algorithms that calculate location probability using probabilistic radio maps belong to the probabilistic positioning algorithm category.

The probabilistic positioning algorithms estimate the location of a fingerprint o^* scanned from a device by finding a location l that maximizes the Bayesian equation:

$$\Pr(l \mid o^*) = \frac{\Pr(o^* \mid l)\Pr(l)}{\Pr(o^*)} \tag{1}$$

where $\Pr(l)$ encodes prior knowledge about where a device may be. On the other hand, the deterministic positioning algorithms compare similarities between fingerprints to find the nearest fingerprints of a given input fingerprint in a radio map. Euclidean distance, Manhattan distance, and Cosine distance can be used for this purpose [31].

III. Signal Fluctuation Matrix

Traditionally, the pattern of RSS distribution has been constructed for every AP at each location [16]. This strategy requires a large amount of samples at each location in order to obtain a complete distribution of RSSs, and then to construct a reliable RM. Here, we propose a novel radio map model called SFM that requires only a few fingerprint samples in the distribution modeling. The SFM ignores the differences in RSS distribution patterns among APs and locations, and it only considers the probability of a fluctuation between each pair of RSS values at a location. The universal pattern of the fluctuations is represented in a two-dimensional matrix, SFM. Because the fluctuation between a particular pair of RSS values can be observed from multiple APs at many locations, a reliable SFM can be constructed even if a small number of samples have been collected at each location.

Suppose that an area of interest is divided into 10 locations; 10 APs are installed in the area; and 5 measurement samples have been collected at each location. In this case, only 5 samples can be used to build RSS distributions for a location in conventional distribution-based radio map models. Meanwhile, 1000 pairs of RSS values are observed from the same data set (10 APs $\times$ 10 locations $\times$ 10 RSS pairs from 5 samples), and can be used for training an SFM. Consequently, the SFM-based radio map model can efficiently cope with the lack of training data.

The SFM is created in the following way. When two or more training samples are collected at a location, and their RSSs from the same AP are different, it is considered that there is a signal fluctuation. The probabilities of the signal fluctuation can be expressed in log-odds scores. We define the score for RSSs i and j by

$$s_{ij} = \log\left(\frac{P(i,j)}{P(i)P(j)}\right),\ i \geq j\ (i,j \in SS) \tag{2}$$

where SS is the set of all possible RSS values, $P(i,j)$ is the observed fluctuation probability of an RSS pair (i,j), and $P(i)P(j)$ is the expected fluctuation probability of the pair.

The observed fluctuation probability is the probability of observing the RSS pair (i,j) for an AP at a location. The expected fluctuation probability is defined by the multiplication of $P(i)$ and $P(j)$, assuming the RSS values are independent of each other. The probabilities $P(i,j)$, $P(i)$, and $P(j)$ are calculated from their occurrence frequencies in a given radio map. For example, when the RSSs from an AP at a location are -30, -30, -40, and -45 dBm, the observed fluctuation probability of an RSS pair (-30, -40) becomes (2/6), and their expected fluctuation probability becomes (2/4) $\cdot$ (1/4).

Fig. 2 shows an example SFM constructed by (2). Both dimensions of the matrix represent RSS values, and the elements represent the probability of signal fluctuation between RSS i and RSS j calculated by (2). The example SFM informs that the pairs with strong signals (the down right side of the matrix) usually have high possibilities to be observed in a location, whereas the pairs with weak signals (the up left side of the matrix) have lower possibilities.

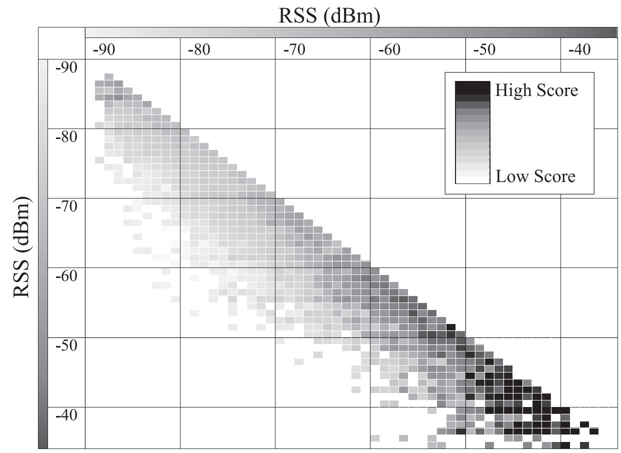

Fig. 2. Example of SFM.

In the positioning phase, the location of an online fingerprint is estimated as the location that has the most similar average fingerprint by using an SFM-based similarity measure. Therefore, another two-dimensional matrix storing mean RSSs for each location is needed for the SFM-based positioning. The SFM-based similarity between an online fingerprint, A, and the average fingerprint of a location, B, is calculated by averaging the SFM scores (2) of all of the RSS pairs from A and B, given by (3), shown at the bottom of the page, where AP_x is the set of APs detected in a fingerprint x, and a_k and b_k are the RSSs of a particular AP k in fingerprints A and B, respectively. Here, an SFM score $s_{a_k \| b_k}$ is interpreted as $s_{a_k b_k}$ if $a_k \geq b_k$, and $s_{b_k a_k}$ otherwise.

From a cost-efficiency point of view, the SFM model has advantage over the other conventional models. Instead, the precision of SFM could be worse than that of histogram and Gaussian distribution-based radio map models because the distribution patterns of signals from each AP at each location are ignored in SFM. However, in some aspects the SFM-based model can achieve a comparable performance to the Gaussian and histogram models.

First, there is a high correlation between the SFM-based similarity score of a pair of fingerprints and their physical distance. When the correlation coefficients (CC) between the similarity score and the physical distance were measured in a simple experiment, the CC of the SFM-based similarity measure was 0.624, which was much higher CC than those of ED, 0.399, Manhattan distance, 0.356, and Cosine distance, 0.380. This indicates that the SFM-based method has higher probability of finding nearest fingerprints to an on-line measurement than the

$$\mathrm{Sim}(A,B) = \frac{\sum_{k \in \mathrm{AP}_A \cap \mathrm{AP}_B} s_{a_k \| b_k} + \sum_{k \in \mathrm{AP}_A - \mathrm{AP}_B} m_{a_k} + \sum_{k \in \mathrm{AP}_B \cap \mathrm{AP}_A} m_{b_k}}{|\mathrm{AP}_A \cup \mathrm{AP}_B|} \tag{3}$$

other methods. The high correlation is an indication that the signal fluctuation patterns have been efficiently reflected in the SFM, and the information of SFM is effectively used in the similarity measure. This has become possible because the SFM is constructed by using enough training samples by ignoring the factors of location and individual AP, and focusing solely on signal fluctuation.

Second, the original purpose of devising the SFM was to handle signal vectors including some errors. Actually, many errors are usually included in fingerprints because of signal fluctuation and some environmental factors. As the errors are reflected into the elements of SFM, they can be handled more efficiently by the SFM than by the other methods.

IV. Mapping of Radio Maps Into Positioning Algorithms

The developers of positioning systems have to choose an appropriate radio map model and positioning algorithm, considering the amount of collected fingerprint samples. However, the amount of samples is not the only factor to be considered in selecting the model and algorithm. The regularity of the sample collection should also be considered, because, with only the amount of samples, it cannot be guaranteed that enough fingerprints have been collected at each location for constructing a particular radio map model. The regularity is usually determined by fingerprint collection methods.

To consider the two factors more formally, we classify the sets of fingerprint samples into five types depending on the fingerprint collection methods and the average number of samples collected at each location. The classification of fingerprints can be different if the purpose of classification is different. The primary purpose of this classification is the mapping of radio map types into radio map model and positioning algorithms. Although a set of samples is the input, and a radio map is the output of modeling, we use the term, radio map, to represent both of them in this paper for simplicity. The five types of radio maps and the detailed conditions of the each type are as follows:

- **Regular-highly-dense radio map**: point-by-point calibration, $n > 20$, where n is the number of fingerprint samples collected at each location.
- **Regular-dense radio map**: point-by-point calibration, $20 \geq n > 10$.
- **Regular-compact radio map**: walking survey, $n \geq 2$.
- **Regular-sparse radio map**: walking survey, $n < 2$.
- **Irregular radio map**: crowdsourcing, **Irregular-dense**, $n \geq 15$, **Irregular-sparse**, $n < 15$.

Fig. 3 shows the mapping of radio map types into radio map models and then positioning algorithms. As shown in the mappings, if a radio map is constructed by point-by-point calibration, collecting more than 20 fingerprint samples at each location, the radio map is classified as a regular-highly-dense radio map. Any kind of radio map model can be used to represent the characteristics of a regular-highly-dense radio map, and hence any kind of positioning algorithms can be used for the regular-highly-dense radio map.

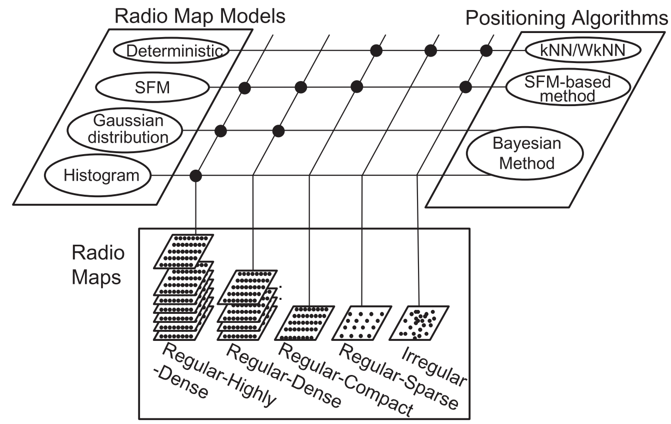

Fig. 3. Mapping of radio maps into radio map models and positioning algorithms.

If a radio map is constructed by point-by-point calibration, with 10 to 20 samples at each location, the radio map is classified as a regular-dense radio map. The deterministic, SFM, and Gaussian radio map models can be used to represent the characteristics of a regular-dense radio map. However, the histogram and kernel models are not suitable for the radio map because of the lack of collected samples.

On the other hand, if a radio map is constructed by a walking survey, collecting only one fingerprint at each measurement point, the radio map is classified as a regular-sparse radio map. Only the deterministic radio map model can be used to represent the characteristics of a regular-sparse radio map. The deterministic positioning algorithms, kNN or WkNN, must be used for the regular-sparse radio map.

When two or more training samples are collected at each location or partitioned area by a walking survey, the SFM-based radio map model and the deterministic radio map model can be used. In general, as more effort is involved in constructing radio maps, more flexibility is allowed in selecting radio map models and positioning algorithms.

When training samples have been collected by crowdsourcing, an irregular radio map is constructed. The irregular radio map is divided into irregular-dense and irregular-sparse radio maps, depending on the number of samples collected at a location. The deterministic, Gaussian, and SFM-based radio map models can be used for the irregular radio map. The positioning algorithms corresponding to the selected radio map models should be used.

V. Evaluation

Four experiments were conducted to evaluate the performance of radio map construction methods: three in the N5 building and on the seventh floor of N1 building, KAIST, Daejeon, and one each at two outdoor environments, an outdoor shopping area in Seoul and a residential area in Daejeon.

The first experiment compared the performance of radio maps constructed by three radio map construction methods in indoor environments. The radio maps were constructed using a point-by-point manual calibration method, a semi-supervised learning-based method, and an unsupervised learning-based

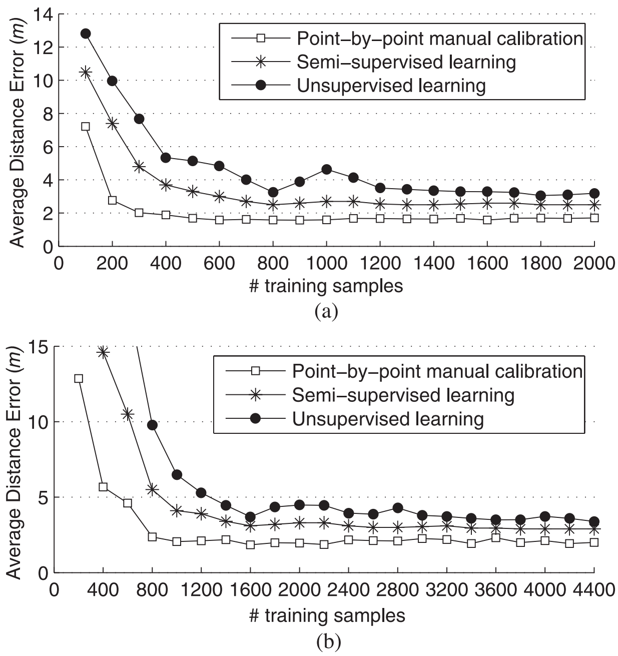

Fig. 4. Positioning accuracies of four radio map construction methods. (a) Accuracy achieved on the seventh floor, N1 building, KAIST. (b) Accuracy achieved in N5 building, KAIST.

method. The positioning accuracy on each radio map was then measured with increment of the number of fingerprint samples.

The second experiment was conducted to compare the performance of the radio map models. The performance of deterministic and probabilistic positioning algorithms such as the kNN, Gaussian, and histogram methods was compared with variation of the number of fingerprint samples collected at each point. The third experiment was conducted to measure the cost of radio map construction methods. The last experiment was performed to evaluate the performance of radio maps constructed in two outdoor environments. The performance of radio maps constructed by the walking survey was compared with that of two different semi-supervised learning methods and the GPS.

A. *Performance Evaluation of Fingerprint Collection Methods*

The experiments were conducted in N5 building and on the seventh floor of N1 building, KAIST, Daejeon, Korea. Three kinds of radio maps were constructed at the experimental areas using the point-by-point manual calibration, semi-supervised learning-based [14], and unsupervised learning-based [14] methods. A Samsung Galaxy S3 was used to collect training data with a sampling rate of 1 Hz. The positioning accuracy of each method was measured with increment of training data. A simple kNN method $(k = 3)$ with Euclidean distance metric [4] was used for the localization test in the evaluation.

Approximately 2000 training samples were collected on the seventh floor, N1 building, and approximately 4400 samples in N5 building for each method. Fig. 4(a) and (b) shows the evaluation results on the seventh floor of N1 building and in N5 building, respectively. When 400 data were used for the learning for the seventh floor of N1 building, the point-by-point manual calibration achieved an accuracy of 1.9 m; the semi-supervised learning, 3.7 m; and the unsupervised learning, 5.3 m. The accuracy gradually improved, and the improvement was saturated with the increment of the learning data for all methods. The radio map types also converted from a sparse, to a compact, to a dense, and then to a highly dense radio map with increment of the number of training samples. When 2000 samples were used, the point-by-point manual calibration achieved an accuracy of 1.7 m; semi-supervised learning, 2.5 m; and unsupervised learning, 3.2 m. The results of the walking survey were not included in the graph because it exhibited only slightly worse performance than the point-by-point method.

Similar results were obtained in N5 building. When 1,400 learning data were used, the point-by-point manual calibration achieved an accuracy of 2.2 m; semi-supervised learning, 3.3 m; and unsupervised learning, 4.5 m. When 4400 learning data were used, the point-by-point manual calibration achieved an accuracy of 2.0 m; semi-supervised learning, 2.9 m; and unsupervised learning, 3.4 m.

Although the semi-supervised and unsupervised learning achieved accuracies slightly worse than the manual calibrations, the results were promising because they were within the accuracy range that can be used by practical positioning systems.

B. *Performance Evaluation of Radio Map Models*

It is known that the positioning accuracy is closely related to the amount of training data collected at each measurement point or partitioned area. However, to our knowledge, the relation between the accuracy and the number of samples collected at each point or partitioned area has not yet been studied in a comprehensive manner. We collected as many as 400 fingerprint samples at each of 70 locations on the seventh floor, N1 building, KAIST to evaluate the accuracy of each radio map model. The accuracies were measured varying the number of training samples from 1 to 400 at each location.

Fig. 5 shows the downward trend of average positioning errors when the number of training samples increases. Since the samples were collected in a noisy signal environment, the increase of the number of samples did not always enhance the positioning accuracy. As a result, some deviations from the trend were observed in the experiment, especially when a few samples were used. However, overall, the positioning results became more accurate and less variable as more samples were available for the training.

When we compared the four methods, the deterministic positioning algorithm using the Euclidean distance (ED) achieved the best results in accuracy when fewer than 10 samples were collected at each location for training. However, only a marginal accuracy improvement was observed with the increment of the training samples. The probabilistic methods (the Gaussian, histogram, and SFM) did not provide usable results when only a few training samples were available; however, the accuracy improved with increment of the training data. The Gaussian method outperformed the ED method when more than 16 training samples were used, and the histogram outperformed the ED and the Gaussian methods when the number of samples exceeded 180 and 320, respectively. This indicates that the two probabilistic methods, the Gaussian and

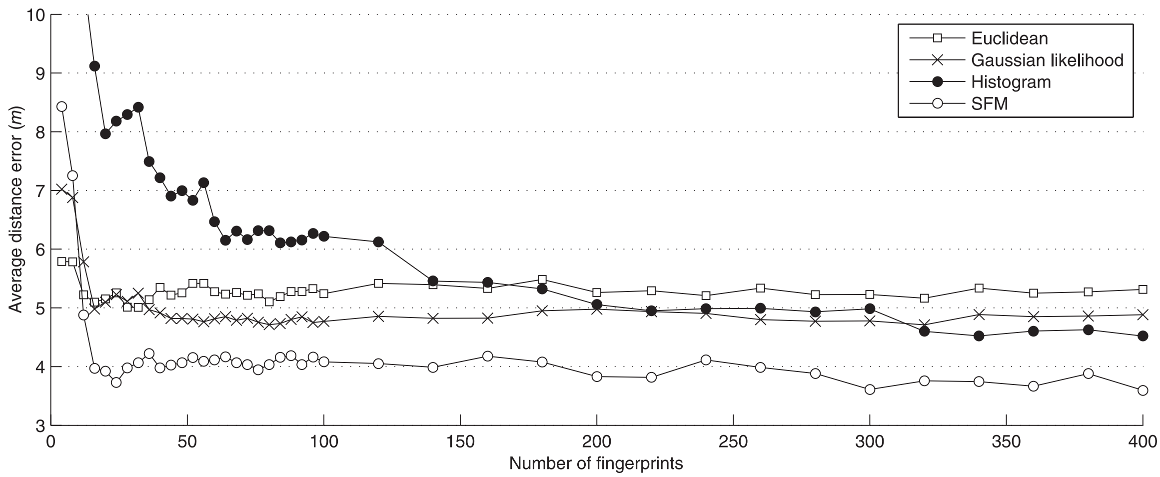

Fig. 5. Average error distances of the radio map models with the increment of training data.

histogram, require many samples to build a reliable radio map model.

The SFM radio map model requires significantly fewer samples to build its matrix compared with the Gaussian and histogram models. As seen in Fig. 5, the SFM-based similarity measure outperformed the others when more than 10 samples were used, and the accuracy improved with increment of the training data. Moreover, the slope of the accuracy improvement was much steeper than that of the other methods, and it achieved the highest accuracy when the number of samples was in a range of 10 to 400. One reason that the SFM achieved such.

The size of a radio map model can become an issue when the model will cover most buildings all over the world. The size complexity of the deterministic model is $O(n)$, where n is the number of locations. The size complexity of the Gaussian model is $O(2n)$. The size complexity of the histogram model is $O(nm)$, where m is the number of divided signal strengths. Because Wi-Fi signal strength is usually divided into approximately 100 different ranges, the value of m can be set to 100. The radio map size for the histogram model is thus approximately 100 times larger than that of other models. This can seriously affect the performance of positioning systems that have to deal with the indoor positioning service of many buildings. The size complexity of the SFM-based method is $O(m)$, where m is the number of divided signal strengths.

C. The Cost of Constructing Radio Maps

The cost of constructing radio maps can be divided into two parts: manual cost and computational cost. The manual cost can simply be estimated by the time required for fingerprint collecting and labeling activities. However, in this study, the manual cost excludes the time for collecting unlabeled fingerprints, because the unlabeled data are assumed to be collected via crowdsourcing without explicit efforts. The computational cost is the time taken for the automatic labeling of fingerprints through semi-supervised or unsupervised learning methods. In the experiments, the computational time for the learning was measured on a computer equipped with a 3.40-GHz Intel Core i7 CPU with 8 GB of memory.

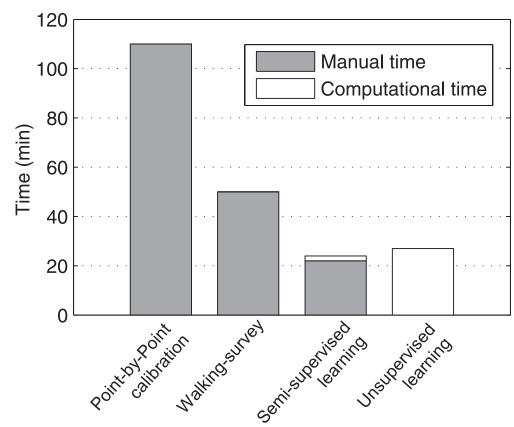

Fig. 6. Contrast of the manual and computation time of the four radio map construction methods.

The time for the four radio map construction methods, the point-by-point calibration, the working survey, the semi-supervised learning, and the unsupervised learning method, was measured using fingerprint samples collected on the seventh floor, N1 building, KAIST. For a fair comparison, all the methods were assumed to use the same number of samples; 2000 samples were used for each method. In the case of the point-by point manual calibration, 20 samples were collected at each location after dividing the experimental area into 100 locations.

Fig. 6 contrasts the manual time and the computational time of the four methods. As shown in the figure, the point-by-point manual calibration required as much as 1 hour and 55 minutes to collect 2000 fingerprint samples, whereas it took approximately 50 minutes to collect the same number of samples by the walking survey. This is because the point-by-point manual calibration requires more effort than the walking survey does in the labeling of fingerprints. The difference between the manual times taken by the two methods indicates that the cost of fingerprint labeling could exceed that of collecting. The computational cost of the point-by-point manual calibration and the walking survey was ignored because it was too small to be considered.

Typically, the semi-supervised learning-based method requires approximately 10% to 60% of the labeled samples

TABLE I
FORMULATION OF MANUAL AND COMPUTATIONAL COSTS OF RADIO MAP CONSTRUCTION METHODS

Method	Manual time	Computational time
Point by point manual calibration	$N_l T_l + N_f T_f$	-
Walking survey	$N_s T_s + N_f T_f$	-
Semi-supervised learning	$N_l T_l + N_f T_f$	$N_i N_l N_u$
Unsupervised learning	-	$N_g N_p N_i N_l N_u$

N_l = the number of locations; T_l = the time taken to recognize a location; N_f = the number of labeled fingerprint samples; T_f = the time taken to measure a sample; N_s = the number of survey lines; T_s = the time taken to recognize a survey line; N_i = the number of iterations in the semi-supervised learning; N_u = the number of unlabeled fingerprint samples; N_g = the number of generations in the unsupervised learning; N_p = the number of populations in the unsupervised learning.

compared with the point-by-point manual calibration for learning [26]. In this study, we assumed that 20% of the point-by-point by manual calibration was used for labeled samples; 400 labeled samples and 1600 unlabeled samples were used for the semi-supervised learning. As a result, the manual cost of the semi-supervised learning was estimated at one-fifth of the time for the point-by-point calibration. Meanwhile, the computational time for the semi-supervised learning was approximately 50 seconds.

The manual cost of the unsupervised learning method was assumed to be zero because it did not require labeled fingerprint samples. Instead, the computational time of the unsupervised learning increased with increment of the unlabeled samples. When the number of samples was 2000, it took approximately 27 minutes.

A considerable amount of computation time is required for the unsupervised learning-based method to achieve accuracy comparable to that of the manual calibration. Despite the computational cost, the construction of radio maps can be automated by the unsupervised learning method because manual labeling is unnecessary. As illustrated in the graph in Fig. 6, the manual labeling cost of point-by-point manual calibration can be converted into computational cost by the unsupervised learning method.

The manual and computational costs of the four methods are formulated as the equations listed in Table I. As shown in the table, the manual time for the point-by-point manual calibration and the walking survey is formulated by similar equations. The difference between the two equations is the first part which represents the time they spend for the fingerprint labeling. Surveyors should recognize every location to label fingerprint samples with correct locations when they are using point-by-point manual calibration, and thus time $N_l T_l$ is required for the fingerprint labeling, where N_l is the number of locations and T_l is the time taken by a surveyor to recognize a single location. Similarly, in the walking survey, the fingerprint labeling is accomplished by recognizing every survey line, and it takes time $N_s T_s$ where N_s is the number of survey lines and T_s is the time taken to recognize a survey line. However, time $N_s T_s$ is typically shorter than $N_l T_l$ in reality because the number of survey lines is usually much smaller than that of locations.

(a) (b)

Fig. 7. Experimental areas. (a) Testbed A1: an outdoor shopping area, Chong-ro, Seoul. (b) Testbed A2: a residence area, Jeonmin-dong, Daejeon, South Korea.

The labeled data for the semi-supervised leaning have been collected by point-by-point manual calibration. Therefore, their manual cost can be formulated by the same equation as shown in Table I. The table also shows the computational time required for the semi-supervised and unsupervised learning methods, which has been reported in the literature [14]. Computational time for a learning-based radio map construction depends on the algorithm adopted by its learning. If a more sophisticated learning algorithm is used, the computational time decreases.

D. Performance Evaluation of Outdoor Radio Maps

Radio maps can be constructed in outdoor environments as well to reduce the GPS positioning error, especially in urban street canyons where the GPS satellite signals are occasionally blocked by high-story buildings. We evaluated the performance of radio maps constructed at an outdoor residence area, Jeonmin-dong, Daejeon, and an outdoor shopping area, Chong-ro, Seoul. Fig. 7(a) depicts the shopping area (testbed A1), and Fig. 7(b) shows the residential area (testbed A2).

Three radio maps were constructed using a walking survey, and two semi-supervised learning methods. The collectors carrying a wireless device (Nexus 5) walked along the streets three times and collected user traces consisting of RSS measurements with a sampling rate of 1 Hz. The ground-truth coordinates of each measurement were obtained by referring to landmarks such as corners and dead ends. Approximately nine-tenths of the collections were used for the calibration and the rest were left for the localization test. Table II is a summary of the testbeds and collected data. The GPS signals were collected together with the fingerprint samples during the walking survey. The GPS signals collected with the samples were used for the location references for the two semi-supervised learning methods. The semi-supervised learning method labeled locations of collected samples using the Segmental K-means (SK) algorithm, which is a well-known local optimization algorithm [13]. Only local optimization was performed without a global search in SK-based semi-supervised learning. The other semi-supervised learning integrated a global search with the SK algorithm within a hybrid learning framework. A memetic

TABLE II
EXPERIMENTAL SETUPS AT TWO AREAS IN DAEJEON AND SEOUL

Testbed	**Area Size**	**Total length of streets**	**# APs detected**	**Data collection**			
				Training data		*Test data*	
				# traces	*# measurements*	*# traces*	*# measurements*
A1	1,800m^2	660m	1,733	56	1,479	7	679
A2	3,300m^2	702m	1,479	20	1,349	6	485

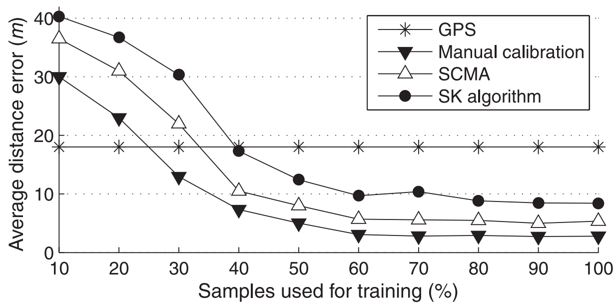

Fig. 8. Effect of the amount of training data on positioning accuracy in testbed A1.

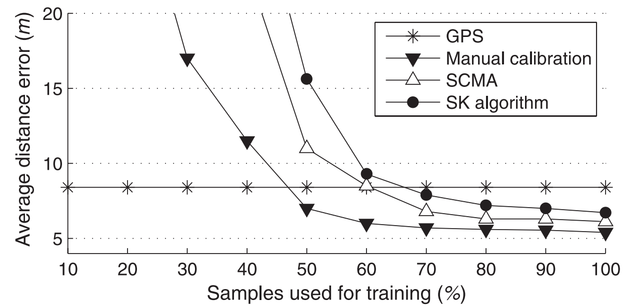

Fig. 9. Effect of the amount of training data on positioning accuracy in testbed A2.

algorithm was used for the global search of the semi-supervised learning [13], and hence we call the method Semi-supervised Calibration using a Memetic Algorithm (SCMA).

The performance of GPS and the constructed radio maps was respectively measured with increment of the learning data. Fig. 8 shows the results of the performance evaluation at testbed A1. As shown in the figure, the manual calibration achieved an average positioning error of less than 3 m, outperforming the other methods regardless of the amount of training data. SCMA, using 1479 training samples with 150 GPS-labeled samples that constituted 10% of the samples, achieved an average positioning error of less than 5.34 m. The accuracy was gradually improved with increment of the training samples, but the improvement was saturated when the number of training samples reached approximately 887, which was approximately 60% of the samples.

In contrast, SK semi-supervised learning achieved an accuracy of 8.41 m, in the same condition. The global search of SCMA further improved the accuracy of SK semi-supervised learning by approximately 30%. Since the error of GPS positioning at A1 was about 18 meters, SCMA achieved 70%, and SK semi-supervised learning 54%, better performance than GPS positioning could achieve.

Fig. 9 shows the results of the performance evaluation at testbed A2. The experiment performed at testbed A2 showed slightly different results from that performed at testbed A1. This is because A2 is an ordinary street with small GPS positioning errors, whereas A1 is an urban street canyon with large GPS positioning errors. As shown in Fig. 9, the manual calibration achieved an average positioning error of less than 5.4 m, also outperforming the other methods regardless of the amount of training data. SCMA, using 1349 training samples with 140 GPS-labeled samples that constituted 10% of the samples, achieved an average positioning error of less than 6.12 m.

In contrast, the SK semi-supervised learning achieved 6.74 m accuracy, in the same condition. The global search of SCMA further improved the accuracy of SK semi-supervised learning by approximately 10%. Like the case at A1, the accuracy gradually improved with the increment of training samples, but the improvement was saturated when the number of training samples reached approximately 809, which was 60% of the samples. Because the error of GPS positioning at A2 was 8.39 m, SCMA achieved only 27%, and SK semi-supervised learning showed 20% better performance than the GPS positioning, respectively.

VI. CONCLUSION

This study compared the performance of radio map construction methods both in indoor and outdoor environments. Despite the evolution of radio map models and fingerprint collecting and labeling methods, no method outperformed other methods in all conditions and situations. The developers of positioning systems have to make wise decisions on choosing radio map models and construction methods considering the cost and performance of these systems.

It was found that the radio map model is a critical factor influencing the performance of radio maps, along with the number of training samples collected at each location. The performance of radio maps varied by the choice of radio map models even if the same number of samples was collected in the same signal environments. Thus, the selection of radio map models should be prudently made considering the number of samples collected at each location or partitioned area. The performance results in this paper will provide information for those who make correct decisions on the models and methods.

The radio map construction methods are still in the process of evolution. The SFM-based radio map model is one example. This work also confirmed the evolution direction of radio map construction methods, from local to global, and from manual to automatic.

References

[1] M. G. Puyol, D. Bobkov, P. Robertson, and T. Jost, "Pedestrian simultaneous localization and mapping in multistory buildings using inertial sensors," *IEEE Trans. Intell. Transp. Syst.*, vol. 15, no. 4, pp. 1714–1727, Jan. 2014.

[2] X. Cheng, L. Yang, and X. Shen, "D2D for intelligent transportation systems: A feasibility study," *IEEE Trans. Intell. Transp. Syst.*, vol. 16, no. 4, pp. 1784–1793, Aug. 2015.

[3] M. B. Kjærgaard, "A taxonomy for radio location fingerprinting," in *Location-and Context-Awareness*. Heidelberg, Germany: Springer, 2007, pp. 139–156.

[4] D. Han, S. Jung, and G. Yoon, "Building a practical Wi-Fi-based indoor navigation system," *IEEE Pervasive Comput.*, vol. 13, no. 2, pp. 72–79, Apr. 2014.

[5] D. Han, S. Lee, and S. Kim, "KAILOS: KAIST indoor locating system," in *Proc. IPIN*, 2014, pp. 615–619.

[6] J. J. Pan, S. J. Pan, J. Yin, L. M. Ni, and Q. Yang, "Tracking mobile users in wireless networks via semi-supervised colocalization," *IEEE Trans. Pattern Anal. Mach. Intell.*, vol. 34, no. 3, pp. 587–600, Mar. 2012.

[7] D. A. Tran and P. Truong, "Total variation regularization for training of indoor location fingerprints," in *Proc. MiSeNet*, 2013, pp. 27–32.

[8] S. Sorour, Y. Lostanlen, S. Valaee, and K. Majeed, "Joint indoor localization and radio map construction with limited deployment load," *IEEE Trans. Mobile Comput.*, vol. 14, no. 5, pp. 1031–1043, Jul. 2014.

[9] K. Chintalapudi, A. Padmanabha, and V. N. Padmanabhan, "Indoor localization without the pain," in *Proc. MobiCom*, 2010, pp. 173–184.

[10] H. Wang, S. Sen, A. Elgohary, M. Farid, M. Youssef, and R. R. Choudhury, "No need to war-drive: Unsupervised indoor localization," in *Proc. MobiSys*, 2012, pp. 197–210.

[11] A. Rai, K. K. Chintalapudi, V. N. Padmanabhan, and R. Sen, "Zee: Zero-effort crowdsourcing for indoor localization," in *Proc. MobiCom*, 2012, pp. 293–304.

[12] C. Wu, Z. Yang, and Y. Liu, "Smartphones based crowdsourcing for indoor localization," *IEEE Trans. Mobile Comput.*, vol. 14, no. 2, pp. 444–457, Apr. 2014.

[13] C. Wu, Z. Yang, Y. Liu, and W. Xi, "Will: Wireless indoor localization without site survey," *IEEE Trans. Parallel Distrib. Syst.*, vol. 24, no. 4, pp. 839–848, Apr. 2013.

[14] S. H. Jung, B. Moon, and D. Han, "Unsupervised Learning for Crowdsourced indoor localization in wireless networks," *IEEE Trans. Mobile Comput.*, vol. 15, no. 11, pp. 2892–2906, Nov. 2016.

[15] P. Kontkanen, P. Myllymaki, T. Roos, H. Tirri, K. Valtonen, and H. Wettig, "Topics in probabilistic location estimation in wireless networks," in *Proc. PIMRC*, 2004, vol. 2, pp. 1052–1056.

[16] Y. Gu, A. Lo, and I. Niemegeers, "A survey of indoor positioning systems for wireless personal networks," *IEEE Commun. Surveys Tuts.*, vol. 11, no. 1, pp. 13–32, 2009.

[17] V. Honkavirta, T. Perälä, S. Ali-Löytty, and R. Piché, "A comparative survey of WLAN location fingerprinting methods," in *Proc. WPNC*, 2009, pp. 243–251.

[18] Y. Wen, X. Tian, X. Wang, and S. Lu, "Fundamental limits of RSS fingerprinting based indoor localization," in *Proc. INFOCOM*, 2015, pp. 2479–2487.

[19] S. He and S. H. G. Chan, "Wi-Fi fingerprint-based indoor positioning: Recent advances and comparisons," *IEEE Commun. Surveys Tuts.*, vol. 18, no. 1, pp. 466–490, 1st Quart. 2016.

[20] T. Gallagher, B. Li, A. Kealy, and A. G. Dempster, "Trials of commercial Wi-Fi positioning systems for indoor and urban canyons," in *Proc. ISGNSS Symp. GPS/GNSS*, Qld, Australia, Dec. 1–3, 2009.

[21] N. Patwari, J. Ash, S. Kyperountas, A. Hero, III, R. Moses, and N. Correal, "Locating the nodes: Cooperative localization in wireless sensor networks," *IEEE Signal Process. Mag.*, vol. 22, no. 4, pp. 54–69, Jul. 2005.

[22] H. Wymeersch, J. Lien, and M. Z. Win, "Cooperative localization in wireless networks," *Proc. IEEE*, vol. 97, no. 2, pp. 427–450, Feb. 2009.

[23] A. T. Ihler, J. W. Fisher, III, R. L. Moses, and A. S. Willsky, "Nonparametric belief propagation for self-localization of sensor networks," *IEEE J. Sel. Areas Commun.*, vol. 23, no. 4, pp. 809–819, Apr. 2005.

[24] T. Pulkkinen, T. Roos, and P. Myllymäki, "Semi-supervised learning for WLAN positioning," in *Proc. ICANN*, 2011, pp. 355–362.

[25] B. Ferris, D. Fox, and L. D. Neil, "WiFi-SLAM using Gaussian process latent variable models," in *Proc. IJCAI*, 2007, vol. 7, pp. 2480–2485.

[26] X. Chai and Q. Yang, "Reducing the calibration effort for probabilistic indoor location estimation," *IEEE Trans. Mobile Comput.*, vol. 6, no. 6, pp. 649–662, Jun. 2007.

[27] A. Goswami, L. E. Ortiz, and S. R. Das, "WIGEM: A learning-based approach for indoor localization," in *Proc. CoNEXT*, 2011, p. 3.

[28] K. Kaemarungsi, "Distribution of WLAN received signal strength indication for indoor location determination," in *Proc. ISWPC*, 2006, pp. 1–6.

[29] B. Sklar, "Rayleigh fading channels in mobile digital communication systems. I. Characterization," *IEEE Commun. Mag.*, vol. 35, no. 7, pp. 90–100, Sep. 1997.

[30] L. Chen, B. Li, K. Zhao, C. Rizos, and Z. Zheng, "An improved algorithm to generate a Wi-Fi fingerprint database for indoor positioning," *Sensors*, vol. 13, no. 8, pp. 11 085–11 096, 2013.

[31] J. Torres-Sospedra, R. Montoliu, S. Trilles, Ó. Belmonte, and J. Huerta, "Comprehensive analysis of distance and similarity measures for Wi-Fi fingerprinting indoor positioning systems," *Expert Syst. Appl.*, vol. 42, no. 23, pp. 9263–9278, Dec. 2015.

Suk Hoon Jung received the Ph.D. degree in information and communications engineering from Korea Advanced Institute of Science and Technology (KAIST), Daejeon, South Korea.

He is a Researcher of computer science with KAIST. His research interests include network analytics, machine learning, and their applications to pervasive computing.

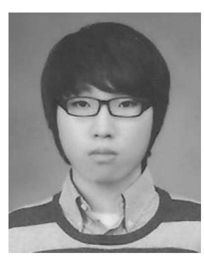

Byeong-Cheol Moon received the M.S. degree in information and communications engineering from Korea Advanced Institute of Science and Technology (KAIST), Daejeon, South Korea. He is currently working toward the Ph.D. degree in information and communications engineering at the KAIST.

His research interests include indoor positioning, mobile computing, and pattern recognition.

Dongsoo Han received the Ph.D. degree in information science from Kyoto University, Kyota, Japan.

He is a Professor of computer science with Korea Advanced Institute of Science and Technology, Daejeon, South Korea. His research interests include indoor positioning, pervasive computing, and location-based mobile applications.